DEPARTMENT OF PHYSICS, UNIVERSITY OF JYVÄSKYLÄ

RESEARCH REPORT No. 6/1999

SHELL-MODEL MATRIX ELEMENTS FOR MUONIC PROCESSES IN LIGHT NUCLEI

BY
TEEMU SIISKONEN

Academic Dissertation
for the Degree of
Doctor of Philosophy

Jyväskylä, Finland
December 1999

URN:ISBN:978-951-39-9496-9
ISBN 978-951-39-9496-9 (PDF)
ISSN 0075-465X

Jyväskylän yliopisto, 2023

ISBN 951-39-0589-6
ISSN 0075-465X

DEPARTMENT OF PHYSICS, UNIVERSITY OF JYVÄSKYLÄ

RESEARCH REPORT No. 6/1999

SHELL-MODEL MATRIX ELEMENTS FOR MUONIC PROCESSES IN LIGHT NUCLEI

BY
TEEMU SIISKONEN

Academic Dissertation
for the Degree of
Doctor of Philosophy

To be presented, by permission of the
Faculty of Mathematics and Natural Sciences
of the University of Jyväskylä,
for public examination in Auditorium FYS1 of the
University of Jyväskylä on December 20, 1999,
at 12 o'clock noon

Jyväskylä, Finland
December 1999

Preface

The work reviewed in this thesis has been carried out during 1996-1999 at the Department of Physics in the University of Jyväskylä.

First of all, I would like to thank my supervisor Prof. Jouni Suhonen for the first-rate guidance and for introducing me to the field of weak interactions. I am also grateful to Prof. (emeritus) Pertti Lipas for introducing me to the nuclear shell-model and few-body quantum mechanics as well as for invaluable comments and advice throughout the work. Thanks belong also to Prof. Juha Äystö and the whole IGISOL group for broadening my interests. Finally, I want to thank Ulla and my parents for their support.

The financial support from the Graduate School of Particle and Nuclear Physics and the University of Jyväskylä is gratefully ackowledged.

Abstract

The nuclear shell-model is used to calculate the nuclear matrix elements for the ordinary muon capture and the muon-electron conversion. In the ordinary muon capture, various residual interactions are applied, and the results are compared to experimental data on capture rates and angular correlations. The renormalized single-particle transition operators are introduced and applied in ^{28}Si and ^{20}Ne. These renormalized operators yield results, which are in better agreement with the predictions coming from the partially conserved axial vector hypothesis than the results obtained with bare operators. The renormalization effects are found to be interaction-independent. Otherwise, different interactions can give very contradictory results.

The single-particle matrix elements with Woods–Saxon radial wave functions are compared to ones obtained with harmonic oscillator radial wave functions. The changes in the capture rates and angular correlation parameters are generally small, and they do not solve the discrepancies between the theory and experiment.

The lepton-flavor violating muon-electron conversion in ^{27}Al and ^{48}Ti is used to restrict the lepton-flavor violating parameters that are included in the extensions of the standard model. Various possible reaction mechanisms are investigated, and channel-by-channel calculations are carried out. The results show that the ground-state to ground-state transition dominates in the two nuclei considered. This increases the possibility of the detection of the muon-electron conversion. In addition, we have separately calculated the vector and axial vector contributions as well as isoscalar and isovector contributions.

List of publications

This thesis is a review of the following publications:

I **Shell-model study of partial muon-capture rates in light nuclei**
T. Siiskonen, J. Suhonen, V.A. Kuz'min, and T.V. Tetereva,
Nucl. Phys. A 635, 446 (1998); Erratum Nucl. Phys. A651, 437 (1999).
https://doi.org/10.1016/S0375-9474(98)00182-1

II **Towards the solution of the C_P/C_A anomaly in shell-model calculations of muon capture**
T. Siiskonen, J. Suhonen, and M. Hjorth-Jensen,
Phys. Rev. C 59, R1839 (1999).
https://doi.org/10.1103/PhysRevC.59.R1839

III **Shell-model effective operators for muon capture in ^{20}Ne**
T. Siiskonen, J. Suhonen, and M. Hjorth-Jensen,
J. Phys. G 25, L55 (1999).
https://doi.org/10.1088/0954-3899/25/8/102

IV **New limits for lepton-flavor violation from the $\mu^- \to e^-$ conversion in ^{27}Al**
T. Siiskonen, J. Suhonen, and T.S. Kosmas,
Phys. Rev. C 60, 62501 (1999).
https://doi.org/10.1103/PhysRevC.60.062501

V **Realistic nuclear matrix elements for lepton-flavor violating $\mu^- \to e^-$ conversion in ^{27}Al and ^{48}Ti**
T. Siiskonen, J. Suhonen, and T.S. Kosmas,
Phys. Rev. C, to be submitted.
https://doi.org/10.1103/PhysRevC.62.035502

VI **Mean-field effects on muon-capture observables**
M. Kortelainen, M. Aunola, T. Siiskonen, and J. Suhonen,
J. Phys. G, in press.
https://doi.org/10.1088/0954-3899/26/2/103

The author of this thesis has written the paper I and participated in the writing of the papers II–VI. The author has written part of the programs used in all the papers and performed the shell-model calculations in all the papers and other numerical calculations in the papers IV and V. The author has participated in the interpretation of the results in all the papers. The author has also made numerous corrections and additions to the shell-model code OXBASH.

Erratum

The experimental error bars plotted in Fig. 2 of the Publication II are wrong. The correct values are given in the text. The corresponding limits are $-2.3 \leq C_P/C_A \leq 5.4$ for the unrenormalized operators and $0.9 \leq C_P/C_A \leq 7.6$ for the renormalized operators. Also the matrix elements plotted in Fig. 1 of the same publication must be multiplied by the factor given in the erratum to the Publication I, $\sqrt{2}/\sqrt{2J_f+1}$.

Contents

Chapter 1

Introduction

The four known fundamental interactions in nature are gravitational, weak, strong and electromagnetic. Gravitational forces are usually taken into account when macroscopic bodies and their interactions are considered. On the nuclear scale its role is neglible. The strong interaction is responsible for nuclear binding, which keeps protons and neutrons together in the nucleus. The theory of the strong interaction is quantum chromodynamics (QCD), but because of the complicated structure of the theory even the bare nucleon-nucleon interaction has not yet been derived starting from the QCD. Instead, various parametrisations of the nucleon-nucleon potential are usually applied. The infinite-range electromagnetic interaction is crucial for the nuclear structure. Because of the Coulomb repulsion between protons, nuclei with $N > Z$ are favoured. In addition, gamma-ray transitions between the nuclear energy levels are an important way of de-exciting the nucleus. The interaction considered in this work is the weak interaction. Electromagnetic and weak interactions are nowadays believed to be different manifestations of a single, more fundamental, electroweak interaction. When the strong interaction is included in the electroweak model, the standard model of particle physics is obtained. However, this model is not considered as the ultimate theory of particle physics, but as a very successful low-energy region approximation. In this work some processes which violate the conservation laws of the standard model are considered.

Leptons are divided into three separate doublets, so-called families, as follows: the first doublet consists of electron and its neutrino, the second muon and its neutrino, and the third one tau-lepton and its neutrino. Each doublet has also a corresponding antiparticle doublet. The electron, muon and tau-lepton possess a finite mass, whereas the masses of the neutrinos are believed to be small, but not necessary zero. Each lepton family has an associated additive quantum number, the lepton number L_i, where $i = e, \mu$ or τ, defined to be $+1$ for type i lepton, -1 for type i antilepton, and zero for other particles. In the standard model lepton number is a conserved quantity. The building blocks of hadrons (strongly interacting composite particles) are the half-integral-spin quarks. The hadrons are further divided into half-integral-spin baryons (p, n, etc.) and integral-spin mesons (π, ρ, etc.). All the leptons and hadrons experience the weak interaction.

A well-known example of the weak process is the nuclear beta decay $(A, Z) \rightarrow (A, Z \pm 1)$

$+ e^{\mp}$. In addition, electron antineutrino or neutrino is emitted. Closely related processes are the orbital electron capture (EC), $(A, Z) + e_b^- \rightarrow (A, Z-1) + \nu_e$, and the orbital muon capture, where an electron is replaced by a muon and electron neutrino by a muon neutrino. All these decays can be classified into allowed and forbidden ones according to the spin and parity change. For allowed transitions spin can change by 0 or 1 units, and the parities of the initial and final nuclear states must be the same. Other transitions are forbidden (they can be further classified as nth forbidden according to the spin and parity change). The energy release in the ordinary beta decay is roughly 10 MeV at maximum. This energy is divided between the three (two in EC) particles present in the final state, thus producing a continuous spectrum (single peak in EC). The released energy is capable of exciting many final states in the daughter nucleus.

Half-lives $t_{1/2}$, or so-called comparative half-lives $ft_{1/2}$, of the allowed beta-transitions are given by a simple expression

$$ft_{1/2} = \frac{K}{C_A^2 B(\mathrm{GT}) + C_V^2 B(\mathrm{F})}, \tag{1.1}$$

where f is a Fermi function, K is a constant, C_V and C_A are vector and axial vector coupling constants, and $B(\mathrm{GT})$ and $B(\mathrm{F})$ are reduced Gamow–Teller and Fermi matrix elements, respectively. The nuclear physics is hidden in these reduced matrix elements. It is a challenge even for the modern nuclear stucture theories to provide reliable values for these matrix elements. In the muon capture no such a simple expression as (1.1) for half-lives exists. This is due to a large energy release, of the order of 100 MeV, which produces many effects unseen in the beta-decay energy scale. These aspects are discussed in Sec. 3.1. In addition, such a high energy release is capable of exciting nearly all the nuclear energy levels, up to continuum.

In the extensions of the standard model lepton-number violating processes can exist. Experimentally one of the most interesting ones is the negative-muon-electron conversion in the field of the nucleus, $(A, Z) + \mu_b^- \rightarrow (A, Z)^* + e^-$, where we have the same nucleus in the initial and final states. If the final state is the ground state, the reaction channel is called coherent. Otherwise one speaks about incoherent channels. Lepton number conservation is clearly violated, since $L_e^{\mathrm{left}} \neq L_e^{\mathrm{right}}$ and $L_\mu^{\mathrm{left}} \neq L_\mu^{\mathrm{right}}$. Also the muon-positron conversion process is possible. It violates also the total lepton number $L = L_e + L_\mu + L_\tau$ conservation. Experimentally these processes have not been detected. Only the upper limits for the branching ratios have been extracted.

In this series of publications collected together the nuclear stucture aspects of the above mentioned muonic processes are discussed. The involved nuclear matrix elements are calculated using the nuclear shell-model, combined with perturbative techniques for the single-particle matrix elements. The results for half-lives and other quantities are compared with experiment where data has been available. Thus the reliability of the shell-model matrix elements can be examined, and various badly-determined parameters can be restricted.

Chapter 2

Nuclear shell-model

The basic assumption of the nuclear shell-model is the movement of a single nucleon in a mean field produced by the other $A-1$ nucleons. This independent-particle motion is governed by the zeroth-order hamiltonian $H^{(0)} = \sum_{i=1}^{A}[T(i) + U(r_i)]$, where $U(r_i)$ is the single-particle (usually harmonic oscillator) potential, taken to be spherically symmetric. The realistic shell-model hamiltonian includes also the particle-particle correlations, usually restricted to two-body interactions. Then we have $H = H^{(0)} + H^{(1)}$, where the residual interaction is given by

$$H^{(1)} = \sum_{i=k<l}^{A} V(k,l) - \sum_{i=1}^{A} U(r_i). \tag{2.1}$$

The resulting hamiltonian matrix (H) is then diagonalized in the chosen subspace of the full Hilbert space. The results are somewhat dependent on the choice of the single-particle potential $U(r)$: In practice, $H^{(1)}$ is replaced by a genuine two-body interaction, i.e.

$$H^{(1)} = \sum_{i=k<l}^{A} V(k,l). \tag{2.2}$$

This is done self-consistently, if in the Hartree–Fock basis the condition

$$\sum_{h} \langle kh|V|lh\rangle = \langle k|U(r_i)|l\rangle \tag{2.3}$$

is fulfilled. Here h labels the occupied states. Then diagrams containing the single-particle potential $U(r_i)$ are cancelled by the corresponding diagrams of V. One such example is shown in Fig. 2.1. In most shell-model calculations a harmonic oscillator single-particle basis is used and hence the self-consistency condition (2.3) is not fulfilled. However, the harmonic oscillator basis (or Woods–Saxon basis) is close enough to Hartree–Fock basis, so that the corrections are usually rather small. The introduction of the reaction or G-matrix complicates things, since then the double self-consistency is needed [1].

The residual interaction can be obtained in many ways. Simple schematic interactions, like the surface delta interaction (SDI), can give surprisingly good results in many cases.

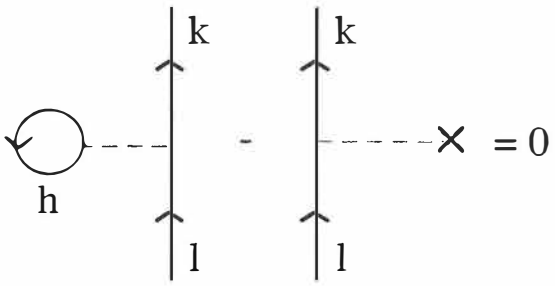

Figure 2.1: One example of the cancellation of the diagrams that are included in Eq. (2.3). The one-particle potential $U(r_i)$ is denoted by a cross.

These kind of interactions have typically only a few free parameters. On the other hand, all the two-body matrix elements and single-particle energies can be fitted to reproduce the selected set of experimental data. The resulting effective (that is, model-space dependent) interaction usually gives a very good description of the nuclei in the region where it was fitted. An example of this kind of approach is the universal sd-shell interaction (USD) by Wildenthal [2]. He fitted all 63 two-body matrix elements and 3 single-particle energies of the sd-shell to the ground-state and low-lying state properties of the selected set of nuclei. In the fit the two-body matrix elements were given an additional mass-dependence. The method in-between (regarding the number of free parameters) is use of the realistic interactions. In this approach, theoretical machinery such as relativistic field theory is used to obtain a general form of the force. Then the free parameters of the model are fitted to experimental nucleon-nucleon scattering data. The infinite repulsive core of the resulting interaction V_{free} must then be removed, since otherwise the perturbative or Hartree–Fock methods can not be applied. This problem can be solved by introducing the short range two-body correlations via reaction (G-) matrix, which takes into account the Pauli principle. In this approach, a certain class of diagrams is selected, namely the ladder diagrams, which are all summed. A formal equation for the G-matrix reads as (assuming that $[Q_{2p}, H^{(0)}] = 0$)

$$G(\omega) = V_{\text{free}} + V_{\text{free}} \frac{Q_{2p}}{\omega - H^{(0)}} G(\omega), \tag{2.4}$$

where $Q_{2p} = 1 - P$ is the Pauli exclusion operator for two-particle channel. It prevents the particles from scattering into occupied states. The G-matrix is a function of the so-called starting energy ω, which is the unperturbed energy of the incoming particles. In Fig. 2.2 the first few ladder diagrams that contribute to G-matrix are shown. The diagrammatic expansion for V_{free} is then written in terms of G, so that no divergent two-particle ladder diagrams are present. If we write

$$V_{\text{free}}(r) \approx V_S(r)\theta(d - r) + V_L(r)\theta(r - d), \tag{2.5}$$

then $G \propto V_L(r)$ to a good approximation. Here V_S is the short-range part of the free-nucleon potential, and V_L is the long-range attractive part. The distance $d \approx 1$ fm [3] is the so-called separation distance, and $\theta(r_1 - r_2)$ is the step function.

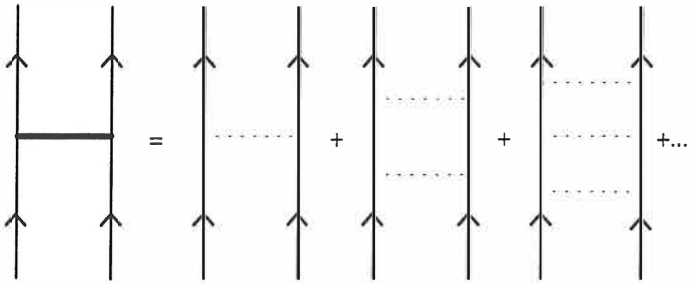

Figure 2.2: First few ladder diagrams that are included in the G-matrix (thick line). The dashed line is the free nucleon-nucleon interaction V_{free}. All the vertical lines are of particle-type.

In this series of works, various residual interactions are used. For pure sd-shell nuclei, like $^{28}_{14}\text{Si}_{14}$, Wildenthal's USD interaction is a standard choice. We have, in addition, used the charge dependent CD-Bonn parametrisation [4, 5] of the modern meson-exchange model together with a G-matrix. In this non-local parametrisation, one-boson-exchange terms are the starting point. Correlated $\pi\pi$ S-wave contribution is included via a fictious one-σ-exchange. As such, the CD-Bonn-based interaction is known to fail in reproducing the spectroscopic properties of e.g. ^{28}Si and ^{28}Al, although the properties of deuteron and triton are very well reproduced [5]. To overcome this problem, some corrections are made to the two-body matrix elements. We have applied the scheme of Zuker [6], where the monopole part of the interaction is removed and then replaced by a phenomenological one. Also the single-particle energies are modified. The monopole part is propotional to the energy centroids

$$E(j_1, j_2) = \frac{\sum_J (2J+1)\langle j_1 j_2 J|V|j_1 j_2 J\rangle}{\sum_J (2J+1)}, \tag{2.6}$$

and it is responsible for the mass-dependence of the single-particle energies ϵ_j and other mean-field properties (it does not include off-diagonal matrix elements of V which are responsible for additional correlations). The other interactions, used in Publication I, include the p-shell interaction PJT by Julies and Richter [7], the cross-shell $p_{1/2}d_{5/2}s_{1/2}$ interaction ZWM [8], the psd-shell interaction WBT [9], and the sd-shell interaction SD-POTA of ref. [10]. The center-of-mass correction is added to the WBT interaction. The ZWM results of Publication I should be considered as rough estimates, since the center-of-mass correction is not included in the wave functions. Our recent tests have shown that the spurious part of the wave functions can be tens of percents for ^{16}O, ^{16}N, ^{20}Ne and ^{20}F with the ZWM interaction.

The modern shell-model codes work either in the m- (uncoupled) or j- (coupled) scheme (Monte Carlo approaches are not discussed in this work). In the m-scheme the basis states do not have good angular momentum. However, the emerging eigenstates have the symmetries of the shell-model hamiltonian, i.e. good angular momentum and parity (and isospin, if an isospin-conserving interaction is used). The disadvantage of this approach are

the large dimensions of the involved hamiltonian matrices, which include all the possible values of angular momenta that can be obtained from the model space. In j-scheme the states with given angular momentum and parity are projected from the m-scheme states. Therefore the hamiltonian matrix is reduced to a block form, where each block has a definite angular momentum and can be diagonalized separately. This way the dimensions are kept tractable. The weak point, however, is the projection, where the numerical errors can make the results unstable. In particular, orthogonality of the basis vectors is very sensitive to rounding errors.

The calculation of the matrix elements of a given one-body operator $\hat{O}$ is done conveniently in the occupation-number representation. Then the reduced matrix element between the many-particle shell-model states can be factorized into single- and many-body parts followingly:

$$(J_f T_f \alpha_f |||\hat{O}|||J_i T_i \alpha_i) = \sum_{j,j'} (j'|||\hat{O}|||j) \frac{(J_f T_f \alpha_f ||| [a^\dagger_{j'} \tilde{a}_j]^J_T |||J_i T_i \alpha_i)}{\sqrt{(2J+1)(2T+1)}}. \tag{2.7}$$

The indices j and j' label the single-particle states. The many-body part, the one-body transition density (OBTD), is the output of the shell-model calculations. For muon-capture operators the single-particle matrix elements of Eq. (2.7) can be calculated analytically, or at least greatly simplified, when harmonic oscillator wave functions are used.

The shell-model code OXBASH [7] was used in our calculations. The code works in the mixed scheme. The hamiltonian matrix is diagonalized in the coupled j-scheme, but the resulting eigenvectors are transformed back to m-scheme. This makes the calculation of the many-body part in Eq. (2.7) much easier. In the nuclei considered in this series of works, the dimensions of the matrices were well below the limits of the code.

Chapter 3

Ordinary partial muon capture

3.1 Form of the interaction

We have adopted the formalism of ordinary (i.e. non-radiative) bound muon capture process

$$(A, Z) + \mu_b^- \rightarrow (A, Z-1)^* + \nu_\mu \tag{3.1}$$

developed by Morita and Fujii in 1960 [11]. They started with the most general form of the hadronic current between the initial proton and final neutron state,

$$C_V\gamma^\alpha + iC_M\sigma^{\alpha\beta}q_\beta + C_S q^\alpha - C_A\gamma^\alpha\gamma^5 - iC_T\sigma^{\alpha\beta}\gamma^5 q_\beta - C_P\gamma^5 q^\alpha. \tag{3.2}$$

This current includes, in addition to familiar vector and axial-vector type interactions of ordinary beta decay, scalar (S), pseudoscalar (P), weak magnetism (M) and tensor (T) couplings. Based on the experiments and expected symmetries of the strong interaction, scalar and tensor couplings are usually set to zero. However, our calculated matrix elements can also be used for the search of the scalar coupling [12]. Furthermore, since the weak magnetism coupling is propotional to the vector coupling, $C_M = C_V(\mu_p - \mu_n)/2M \approx 3.706\, C_V/2M$, we have only three free coupling constants C_V, C_A and C_P in the model.

The vector and axial vector couplings are involved in the ordinary beta decay [see Eq. (1.1)]. In shell-model calculations the nuclear-matter value of the ratio $C_A/C_V = -1.0$ is often used instead of the bare nucleon value, $C_A/C_V \approx -1.25$ ($C_V = 1.0$). In our calculations the value -1.0 was used, based on the test for the beta decay process $^{12}\mathrm{C}(0^+_{\mathrm{g.s.}}) \rightarrow {}^{12}\mathrm{B}(1^+_1)$ and shell-model calculations performed by other authors [13, 14, 15]. The exceptions were the calculations, where the effective transition operators were used. Those are discussed below in Sec. 3.3. In the erratum to Publication I the correct values of the matrix elements are given. In the case of the capture process $^{12}\mathrm{C} + \mu^- \rightarrow {}^{12}\mathrm{B} + \nu_\mu$, these matrix elements seem to favour the use of the bare coupling $C_A/C_V = -1.251$, in contrary to Fig. 3 of Publication I. The rate with $C_P/C_A = 7$, $C_A/C_V = -1.251$ is 6.088×10^3 1/s, in excellent agreement with experiment. However, based on the large set of data coming from the beta decay, the nuclear-matter value of the ratio C_A/C_V should be a good choice.

When the values of the vector and axial vector coupling constants are fixed, the only free parameter is the pseudoscalar coupling C_P. The partially conserved axial vector current hypothesis (PCAC) gives an estimate $C_P/C_A \approx 7$. This value is obtained by investigating the pion vertex corrections to the axial vector matrix element of free-neutron beta decay. The axial vector current of this decay is conserved in the limit $m_\pi \to 0$, hence it is considered only partly conserved. If the axial current were conserved, the decay of free π^- would be impossible.

Various extractions of the ratio C_P/C_A give contradictory results. The value coming from the muon capture in hydrogen gives is $6.8 \leq C_P/C_A \leq 10.6$ [16], in agreement with PCAC. In this case the nuclear matter effects can naturally be neglected. The interesting question arises: is the value of the pseudoscalar coupling renormalized in the nuclear medium in the same way as the axial vector coupling? Realistic nuclear model calculations ([17], Publication I) seem to support this proposition. The authors in ref. [17] give the limits $C_P/C_A = 0.0 \pm 3.2$ (see also ref. [18]). However, such a strong quenching seems unlikely: A rough estimate can be obtained from the nuclear-matter value of C_A, which is renormalized by 20% compared to the free-nucleon value. This would lead to estimate $C_P/C_A \sim 5.6$ with unrenormalized C_A. However, if both coupling constants are renormalized by the same amount, then C_P/C_A should be around 7. Other theoretical estimates are shortly discussed in Publication IV.

3.2 Single-particle operators

Starting from the general form of the baryonic current introduced in Sec. 3.1, the expressions for the single-particle operators can be derived [11]. The usual non-relativistic reduction of nucleon spinors is valid, even though the released energy is high: the recoil energy of the nucleon is few hundred keV's, when the energy release is 100 MeV and $A = 30$. This energy is small when compared to the nucleon mass, roughly 939 MeV. The leptonic part is kept relativistic, only the small component of the bound-muon wave function is discarded (this approximation is valid when $\alpha Z \ll 1$, where α is the fine structure constant). The small components of the muon wave function change the results by a few percent, as pointed out by Gillet and Jenkins [19]. However, other uncertainties in the calculations are much larger than that.

When the lepton wave functions are written in the spherical basis, the sum over magnetic quantum numbers is taken, and the integral over the neutrino momentum is performed, we get in the impulse approximation

$$W = 4P(\alpha Z m'_\mu)^3 \frac{2J_f + 1}{2J_i + 1} \left(1 - \frac{Q}{m_\mu + AM}\right) Q^2 \tag{3.3}$$

for the capture rate from the initial state J_i to the final state J_f. The reduced muon mass is given by m'_μ. The energy release is given by

$$Q = (m_\mu - \Delta M) \left(1 - \frac{m_\mu - \Delta M}{2(M_f + m_\mu)}\right). \tag{3.4}$$

Matrix element	Ψ_s
$[0wu]$	$j_w(qr_s)\mathcal{Y}^{M_f-M_i}_{0wu}(\hat{r}_s)\delta_{wu}$
$[1wu]$	$j_w(qr_s)\mathcal{Y}^{M_f-M_i}_{1wu}(\hat{r}_s,\sigma_s)$
$[0wu\pm]$	$\left[j_w(qr_s) \pm \alpha Z(m'_\mu/p_\nu)j_{w\mp1}(qr_s)\right]\mathcal{Y}^{M_f-M_i}_{0wu}(\hat{r}_s)\delta_{wu}$
$[1wu\pm]$	$\left[j_w(qr_s) \pm \alpha Z(m'_\mu/p_\nu)j_{w\mp1}(qr_s)\right]\mathcal{Y}^{M_f-M_i}_{1wu}(\hat{r}_s,\sigma_s)$
$[0wup]$	$ij_w(qr_s)\mathcal{Y}^{M_f-M_i}_{0wu}(\hat{r}_s)\sigma_s\cdot\mathbf{p}_s\delta_{wu}$
$[1wup]$	$ij_w(qr_s)\mathcal{Y}^{M_f-M_i}_{1wu}(\hat{r}_s,\mathbf{p}_s)$

Table 3.1: Definition of reduced matrix elements for muon capture.

Here ΔM is the mass difference between initial and final states. The quantity P includes all the nuclear physics aspects of the reaction. In particular, all the reduced nuclear matrix elements of the single-particle transition operators are included in it. These many-body matrix elements can be conveniently divided into single- and many-body parts according to Eq. (2.7). We have used harmonic-oscillator and Woods–Saxon basis in calculation of the single-particle matrix elements.

The single-particle operators and the corresponding reduced matrix elements are listed in Table 3.1. The operators are defined via

$$\int U^\dagger_{J_fM_f}\sum_{s=1}^{A} e^{-\alpha Z m'_\mu r_s}\Psi_s\tau^s_- U_{J_iM_i}d\mathbf{r}_1\cdots d\mathbf{r}_A = [k\,w\,u\,(\pm \text{ or } p)](J_i\,M_i\,u\,M_f - M_i|J_f\,M_f). \tag{3.5}$$

The functions $\mathcal{Y}^M_{kwu}$ are vector spherical harmonics and U_{JM} are the nuclear many-body wave functions. The effective charge used by many authors does not enter our equations, since we have used the full muon radial wave function. Effective charges should be used only when the radial wave function is taken to be constant inside the nuclear volume, approximated by its value in the origin.

The single-OBTD dominance, discussed in Publication I, stabilizes the results against the changes in the interaction. In the opposite case the magnitudes of the matrix elements may depend strongly on the type of interaction. This can be readily understood in terms of cancellations between various terms. When all the OBTD's have roughly the same magnitude, the cancellations between various terms in the sum of Eq. (2.7) can easily happen, and the small changes in the transition densities can have a large impact on the resulting nuclear matrix elements.

The angular-intensity distribution of the gamma-rays following the muon capture is given by

$$I(\theta) = I_0[1 + \alpha P_2(\cos\theta)], \tag{3.6}$$

where θ is the angle between the emitted gamma and the muon neutrino. The measurable quantity α is closely related to the angular correlation parameter x, as $\alpha =$

$(\sqrt{2}x - x^2/2)/(1 + x^2)$. Since the emitted neutrino is impossible to detect, sophisticated experimental techniques have been developed (for details, see refs. [17, 18]). The definition of x is

$$x = M_1(2)/M_1(-1), \tag{3.7}$$

where the multipole matrix elements are given by

$$M_1(-1) = \sqrt{\frac{2}{3}}\left\{\left(\frac{1}{3}G_P - G_A\right)[101] + G_P\frac{\sqrt{2}}{3}[121] - \frac{C_A}{M}[011p] + \frac{C_V}{M}\sqrt{\frac{2}{3}}[111p]\right\}, \tag{3.8}$$

$$M_1(2) = \sqrt{\frac{2}{3}}\left\{\left(G_A - \frac{2}{3}G_P\right)[121] - G_P\frac{\sqrt{2}}{3}[101] + \frac{C_A}{M}\sqrt{2}[011p] + \frac{C_V}{M}\sqrt{\frac{2}{3}}[111p]\right\}. \tag{3.9}$$

Above we have defined

$$G_P = (C_P - C_A - C_V - C_M)\frac{E_\nu}{2M},\ G_A = C_A - (C_V + C_M)\frac{E_\nu}{2M}. \tag{3.10}$$

Thus the importance of x is related to its strong dependence on the pseudoscalar coupling C_P. When the experimental data on x is available, Eqs. (3.8) and (3.9) together with Eq. (3.7) can be used for the extraction of the ratio C_P/C_A. Unfortunately, angular correlation measurements are difficult to carry out, and at the moment data exists for ^{28}Si only [17, 18]. There is, however, a plan to do a measurement also in ^{20}Ne [20].

The angular correlation data should be a more reliable way to extract the value of the ratio C_P/C_A than the capture rate data. Comparison of the Eqs. (3.3) and (3.7) shows that the expression for the rate depends on the products of the reduced matrix elements, whereas x is given by the ratios of them. Therefore x should be less sensitive to the systematic errors in the nuclear matrix elements. However, due to the lack of data, the capture rates must be used in the majority of cases.

The single-particle operators include exponentials $\exp(-i\mathbf{q}\cdot\mathbf{r})$, where $|\mathbf{q}| \approx 100$ MeV is the momentum transfer (in the units $\hbar = c = 1$). In the ordinary beta decay the allowed transitions are the ones corresponding to the limit $\exp(-i\mathbf{q}\cdot\mathbf{r}) = 1$, which is the $l = 0$ term in the Fourier–Bessel expansion

$$e^{i\mathbf{q}\cdot\mathbf{r}} = 4\pi\sum_{l,m} i^l j_l(qr)Y_{lm}(\Omega_r)Y^*_{lm}(\Omega_q) \tag{3.11}$$

when $qr \ll 1$. Now, when we have about ten times larger momentum transfer, this approximation is no longer valid. The radial integrals include the oscillating part, and the radial matrix elements may be sensitive to the shape of the radial single-particle wave functions at the nuclear surface. To examine this effect, we have made muon capture calculations using the Woods–Saxon single-particle basis, and compared the results to the oscillator-basis calculations (see Publication VI). These results are summarized in Table 3.2 with $C_P/C_A = 7$, $C_A/C_V = -1.0$.

Parent	J_f^π (Interaction)	$W_{\exp}$ ($10^3\,1/s$)	W_{th} ($10^3\,1/s$)		x	
			h.o.	WS	h.o.	WS
^{12}C	1_1^+(PJT)	6.0 ± 0.4	4.143	3.306		
^{16}O	1_1^-(WBT)	1.31 ± 0.11	2.375	1.431		
	2_1^-(WBT)	8.0 ± 1.2	14.437	12.032		
^{20}Ne	1_1^+(W)	6.32 ± 0.20	1.803	2.258	0.454	0.402
	1_2^+(W)	< 1.32	1.449	0.549	0.586	0.743
	1_1^-(WBT)	6.25 ± 0.13	1.179	0.945		
	2_1^-(WBT)	6.65 ± 0.20	0.289	0.264		
	2_2^-(WBT)	< 4.61	20.408	19.182		
^{23}Na	$1/2_1^+$(W)	4.9 ± 1.4	2.242	1.970		
	$1/2_2^+$(W)	10.4 ± 2.2	3.643	3.098		
	$5/2_1^+$(W)	-	0.348	0.323		
	$5/2_2^+$(W)	2.1 ± 0.5	0.800	0.573		
^{28}Si	1_1^+(W)	14.4 ± 1.8	24.585	22.271	0.470	0.479
	1_2^+(W)	29.7 ± 3.6	2.230	2.158	0.539	0.549
	1_3^+(W)	48.4 ± 3.8	25.836	25.222	0.493	0.491
	1_1^+(SDPOTA)	14.4 ± 1.8	6.514	5.500	0.425	0.441
	1_2^+(SDPOTA)	29.7 ± 3.6	8.233	7.696	0.489	0.498
	1_3^+(SDPOTA)	48.4 ± 3.8	40.909	39.565	0.49	0.494
^{32}S	1_1^+(W)	-	2.619	2.549		
	1_2^+(W)	-	19.447	17.783		
	1_3^+(W)	-	0.157	0.348		
	1_4^+(W)	-	6.345	6.309		

Table 3.2: The comparison of the capture rates W and the angular correlation parameter x in the harmonic oscillator (h.o.) and Woods–Saxon (WS) single-particle bases. The results are calculated with $C_P/C_A = 7$ and $C_A/C_V = -1.0$.

3.3 Effective transition operators

Shell-model calculations are always truncated to a reasonably small valence space. The size of this model space is dictated by physical reasons as well as available computer resources. This truncation introduces the concept of the effective interactions and operators. In Ch. 2 the effective interaction is defined to be dependent on the chosen model space. In the same spirit, effective operators are defined via projections into chosen (finite) model space.

The matrix element of a single-particle operator $\hat{O}$ between the exact wavefunctions $|\Psi_{i,f}\rangle$ of the full Hilbert space, is given by

$$O_{fi} = \frac{\langle \Psi_f | \hat{O} | \Psi_i \rangle}{\sqrt{\langle \Psi_f | \Psi_f \rangle \langle \Psi_i | \Psi_i \rangle}}. \tag{3.12}$$

Since the shell-model calculations are always done in a subspace of the full Hilbert space, we do not know the exact wave functions, only their projections $|\Phi\rangle \equiv P|\Psi\rangle$ into the model space. Therefore we try to construct an effective transition operator $\hat{O}_{\text{eff}}$, which obeys the equation

$$O_{fi} = \langle \Phi_f | \hat{O}_{\text{eff}} | \Phi_i \rangle. \tag{3.13}$$

This effective operator is calculated by using perturbative techniques (for a detailed review see [1]). The diagrams are evaluated up to the second order in a G-matrix obtained from the CD-Bonn interaction. Intermediate state particle-hole excitations are included up to $6\text{–}8\hbar\omega$ in oscillator energy in order to obtain converging results.

The effective operators used with the USD one-body transition densities were also obtained with the CD-Bonn interaction: in perturbation expansion the matrix elements which connect to the states outside the model space are needed, and obviously they are not available for the USD interaction.

Chapter 4

Muon-electron conversion

4.1 Introduction

The existence of the lepton-flavor violating muon-electron conversion

$$(A, Z) + \mu_b^- \rightarrow (A, Z)^* + e^- \tag{4.1}$$

has not been experimentally verified. The experiments have only been able to put upper limits for the branching ratio of the $\mu \rightarrow e^-$ conversion relative to the ordinary muon capture,

$$R_{\mu e^-} = \frac{\Gamma(\mu^- \rightarrow e^-)}{\Gamma(\mu^- \rightarrow \nu_\mu)}. \tag{4.2}$$

These limits can be used to restrict the parameters that enter in the lepton-flavor violating lagrangians. We have considered several possible reaction channels which lead to $\mu^- \rightarrow e^-$ conversion. Typically, these Lagrangians contain only a few parameters related to lepton flavor violation. The branching ratio of Eq. (4.2) for coherent (i.e. ground state to ground state) channel can be factorized as $R_{\mu e^-} = \rho\gamma$, where γ includes all the nuclear physics input, i.e. the transition matrix element. The parameter ρ contains the flavor-violating parameters. The related R-parity symmetry, R_p, discussed in Publications IV and V is introduced in supersymmetric theories in order to eliminate the lepton and baryon number non-conservation. The R-parity is defined as

$$R_p = (-1)^{3B+L+2S}, \tag{4.3}$$

where B, L, and S are the baryon, lepton and spin quantum numbers, respectively. However, R_p-symmetry has no well-motivated theoretical background.

Experimentally the coherent channel is the most important one, since it is free from the background produced by orbital muon capture and other related processes. The relative strength of the coherent channel can be calculated if all the partial conversion strengths are known. Then

$$\eta = \frac{\Gamma_{\mathrm{coh}}(\mu^- \rightarrow e^-)}{\Gamma_{\mathrm{tot}}(\mu^- \rightarrow e^-)} \tag{4.4}$$

is a measure of the relative strength. Clearly, nuclear-structure calculations are needed in order to obtain the transition matrix elements. For the coherent $0^+ \to 0^+$ channel the matrix element can be written in terms of the nuclear form factors $F_Z(q^2)$ and $F_N(q^2)$. These form factors depend on the single-particle level occupation probabilities $(V_j)^2$, which can be obtained from e.g. RPA calculations [21], or from large-scale shell-model calculations (Publication V). The form factors are defined as

$$F_Z = \frac{1}{Z}\sum_j \hat{j}(j\|j_0(qr)\|j)\left(V_j^p\right)^2, \quad F_N = \frac{1}{N}\sum_j \hat{j}(j\|j_0(qr)\|j)\left(V_j^n\right)^2. \tag{4.5}$$

For incoherent channels and other than even-even nuclei the task is more demanding. The two nuclei considered in Publications IV and V, $^{27}_{13}$Al and $^{48}_{22}$Ti, are well-suited for the shell-model treatment. The full sd-shell calculation with the USD interaction [2] was performed for aluminium, and for titanium the Millener–Kurath type interaction in the fp-shell was applied (see the interaction library of [7] and [22]). Test calculations in the fp-shell were carried out with the FPD6 interaction of ref. [23] and the KB3 interaction of ref. [24]. In titanium, particle-hole excitations up to 4p–4h were allowed from the $f_{7/2}$ single-particle orbit. The negative-parity states can not be produced in the chosen model spaces. Previous studies (e.g. RPA calculations of ref. [21]) have shown that their contribution to the incoherent strength is significant. This reduces the value of η slightly, but the value of ρ does not change.

4.2 Transition operator

The Lagrangian for the conversion process is obtained from the Feynmann rules. The related topics are reviewed in ref. [25], and the Feynman rules for the minimal extensions of the standard model are listed in ref. [26]. The resulting transition operator corresponding to the diagrams shown in Fig. 4.1, after the non-relativistic reduction, can be divided in two parts. The vector-, or Fermi, type operator reads

$$\Omega_0 = \tilde{g}_V f_V \sum_{j=1}^{A}\left(3 + \beta\tau_{3j}\right)e^{-i\mathbf{q}_f\cdot\mathbf{r}_j} \tag{4.6}$$

and the axial-, or Gamow–Teller, type operator

$$\mathbf{\Omega} = -\tilde{g}_A f_A \sum_{j=1}^{A}\left(\frac{f_V}{f_A}\beta'' + \beta'\tau_{3j}\right)\frac{\sigma_j}{\sqrt{3}}e^{-i\mathbf{q}_f\cdot\mathbf{r}_j}. \tag{4.7}$$

Parameters $\tilde{g}_V$, $\tilde{g}_A$, β, β' and β'' select the specific reaction channel. The coupling constants $f_A = 1.24$ and $f_V = 1.0$ are the familiar vector and axial vector couplings. Again, Eq. (2.7) was used to separate the single- and many-body matrix elements.

Like in muon capture, the exponential appearing in Eqs. (4.6) and (4.7) can not be approximated by $\exp(-i\mathbf{q}_f\cdot\mathbf{r}_f) \approx 1$ because of the large momentum transfer

$$q_f \equiv |\mathbf{q}_f| = m_\mu - \epsilon_b - E_x, \tag{4.8}$$

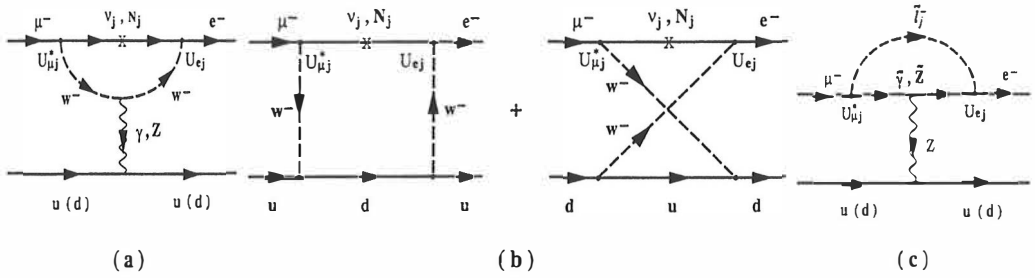

Figure 4.1: Typical Feynman diagrams that contribute to the muon-electron conversion process. Specific mechanisms involving massive intermediate neutrinos are shown. These diagrams correspond to (a) photonic (b) W^--exchange box diagrams and (c) Z-SUSY exchange mechanisms.

where ϵ_b is the atomic 1s-binding energy of the muon. The excitation energy of the final nuclear state is given by E_x. The multipole transition operators are obtained via the Fourier–Bessel expansion of Eq. (3.11). The resulting matrix elements are given by

$$(f\|T^{(l,\sigma)J}\|\text{g.s.}) = \sum_{j_1 j_2} m^{(l,\sigma)J}(j_2 j_1)\left[C^0_\sigma\, D(j_2 j_1; J, T=0) + C^1_\sigma\, D(j_2 j_1; J, T=1)\right], \quad (4.9)$$

where the functions $D(jj'; JT)$ are the one-body transition densities of Eq. (2.7). The angular momentum couplings are included in the coefficients $m^{(l,\sigma)J}$. The coefficients C^T_σ select the reaction channel. The integral over the angle Ω_q has been taken. The total matrix element, in terms of the multipole operators, is now given by

$$\begin{aligned} M^2 &= S_V + 3S_A \qquad (4.10)\\ &= \sum_f \left(\frac{q_f}{m_\mu}\right)^2 \sum_J \left[\left|\left(J_f\|T^{(J,0)J}\|J_i(\text{g.s.})\right)\right|^2 + 3\sum_{l=J,J\pm1}\left|\left(J_f\|T^{(l,1)J}\|J_i(\text{g.s.})\right)\right|^2\right]. \end{aligned}$$

Here S_V is the vector matrix element and S_A the axial vector matrix element.

The monopole ($J = 0$) part of the transition operator in Eq. (4.10) gives a large contribution within the closed shells. To take this into account, no-core shell-model calculations were carried out keeping the shells below the sd-shell (aluminium) or the fp-shell (titanium) closed. The contribution coming from the core is independent of the interaction. In Fig. 4.2 the contributions from the different multipoles in Eq. (4.10) are shown for the photonic $\frac{5}{2}^+ \rightarrow \frac{5}{2}^+$ channel in aluminium. Like in beta-decay and muon capture, the strength decreases for higher multipoles, corresponding to higher forbiddennes of the transition.

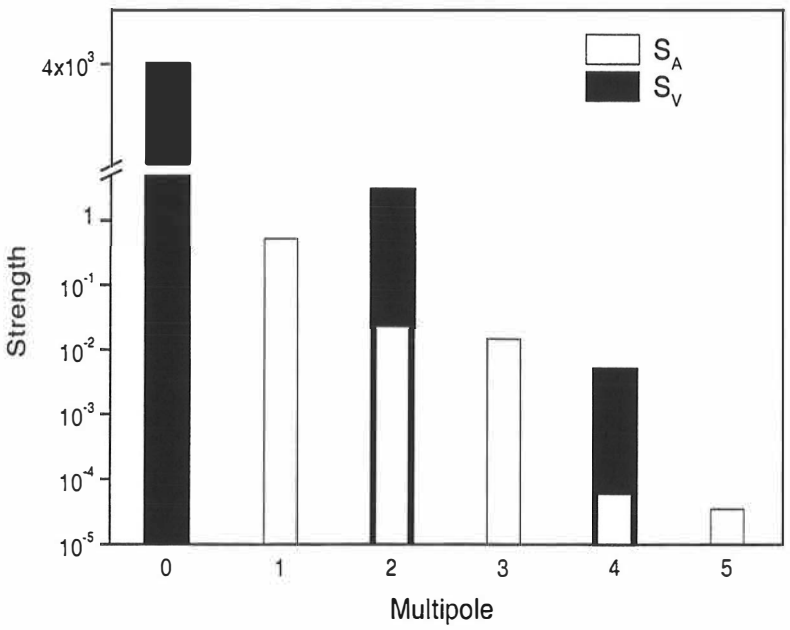

Figure 4.2: Contribution from the different multipoles to the photonic $\frac{5}{2}^+$(g.s.) $\rightarrow$ $\frac{5}{2}^+$ channel in ^{27}Al. The vector and the axial vector contributions are shown separately. The factor $(q_f/m_\mu)^2$ is not included.

Chapter 5

Discussion and conclusions

In the ordinary muon capture process, as well as in muon-electron conversion, the large momentum transfer causes complications when compared to the ordinary beta decay. Firstly, the hadronic current reveals more complex structures when the momentum transfer increases, so that the set of transition operators is enlarged compared to the beta-decay. Secondly, these processes provide good tests to the nuclear structure calculations, since in addition to the allowed transitions, forbidden transitions have been measured in many cases.

The results for muon capture indicate strong interaction dependence. In addition, even in the same nucleus, the interaction can clearly overestimate the rate in one case and underestimate in the other. The renormalized transition operators, introduced in Publications II and III, partly solve this problem. For the angular correlation parameter x of Eq. (3.7), the results clearly get closer to what is expected from the experiments and from the PCAC prediction. The renormalization effects on the transition rates are also clearly seen. Again, in ^{20}Ne we get improvement, whereas in ^{28}Si the rate for 1_3^+ state deviates more from the experiment. However, all these effects are nearly interaction-independent. This is also seen from the matrix elements, where renormalization decreases the magnitude of the matrix elements independently of the interaction. A similar effect can be seen in the beta-decay Gamow–Teller matrix elements, which decrease when the model space increases. Usually, in ordinary beta-decay, this effect is partly included in the so-called Gamow–Teller quenching factor (which includes also other effects like mesonic degrees of freedom). Recent results by Ciechanowicz *et al.* [27] indicate that at least in the case of muon capture in ^{28}Si the mesonic degrees of freedom, perhaps surprisingly, play only a minor role.

The transition operators include the spherical Bessel functions $j_l(qr)$, which oscillate rapidly at the nuclear surface. Therefore, the nuclear matrix elements could be sensitive to the form of the radial part of the wave function. To test this, we have used in addition to the usual harmonic oscillator radial wave functions the Woods–Saxon radial single-particle wave functions. The results are collected in Table 3.2. Unfortunately, the Woods–Saxon basis does not help to solve the discrepancies in the transition rates. A possible refinement could be the use of the renormalized transition operators together with the Woods–Saxon

single-particle basis.

Also the negative-muon-electron conversion is studied in the context of the nuclear shell-model. The transition operators obtained from the extensions of the standard model are used together with the transition densities obtained from the shell-model. The emerging matrix elements are then used to restrict the lepton-flavor violating parameters included in our model lagrangians. We have used the expected sensitivity of the Brookhaven ^{27}Al experiment and the existing data on ^{48}Ti for extraction of the flavor-violating parameter ρ and the parameter η of Eq. (4.4). The operators are written in such a form that the vector and axial vector as well as isoscalar and isovector contributions can be examined separately. The results show that the coherent transition is the dominant channel in ^{27}Al and ^{48}Ti for all the mechanisms considered in Publications IV and V. This is due to a very strong monopole matrix element. In addition, the matrix elements are dominated by vector-isoscalar contribution. The strength of the incoherent channels is strongly concentrated on the low-lying final states. The ground state consists mostly of the Hartree–Fock configuration, whereas the final states with high excitation energies consist mostly of many particle-many hole excitations from this configuration. Thus the overlap between the final states and the ground state with particle-hole type excitations generated by the operator $[a^\dagger_{j'}\tilde{a}_j]^J_T$ of Eq. (2.7) is small when the excitation energy increases. The results are stable against the changes in the residual interaction.

Bibliography

[1] P.J. Ellis and E. Osnes, Rev. Mod. Phys. 49, 777 (1977).

[2] B.H. Wildenthal, Prog. Part. Nucl. Phys. 11, 5 (1984).

[3] M. Hjorth-Jensen, T.T.S. Kuo, and E. Osnes, Phys. Rep. 261, 125 (1995).

[4] R. Machleidt, K. Holinde, and Ch. Elster, Phys. Rep. 149, 1 (1987).

[5] R. Machleidt, F. Sammarruca, and Y. Song, Phys. Rev. C 53, R1483 (1996).

[6] A.P. Zuker, Nucl. Phys. A 576, 65 (1994).

[7] B.A. Brown, A. Etchegoyen, and W.D.M. Rae, The computer code OXBASH, MSU-NSCL report 524, 1988.

[8] A.P. Zuker, Phys. Rev. Lett. 23, 983 (1969); J.B. McGrory and B.H. Wildenthal, Phys. Rev. C 7, 974 (1973).

[9] E.K. Warburton and B.A. Brown, Phys. Rev. C 46, 923 (1992).

[10] B.A. Brown, W.A. Richter, R.E. Jules, and B.H. Wildenthal, Ann. Phys. 182, 191 (1988).

[11] M. Morita and A. Fujii, Phys. Rev. 118, 606 (1960).

[12] V. Egorov, Ch. Briancon, V. Brudanin, J. Deutsch, T. Filipova, J. Govaerts, C. Petitjean, R. Prieels, Yu. Shitov, T. Siiskonen, J. Suhonen, Ts. Vylov, V. Wiaux, I. Yutlandov, and Sh. Zaparov, Proceedings of NANP '99 (JINR, Dubna 1999), *to be published.*

[13] B.L. Johnson, T.P. Gorringe, D.S. Armstrong, J. Bauer, M.D. Hasinoff, M.A. Kovash, D.F. Measday, B.A. Moftah, R. Porter, and D.H. Wright, Phys. Rev. C 54, 2714 (1996).

[14] W.T. Chou, E.K. Warburton, and B.A. Brown, Phys. Rev. C 47, 163 (1993).

[15] B.H. Wildenthal, M.S. Curtin, and B.A. Brown, Phys. Rev. C 28, 1343 (1983).

[16] G. Bardin, J. Duclos, A. Magnon, J. Martino, A. Richter, E. Zavattini, A. Bertin, M. Piccinini, and A. Vitale, Phys. Lett. B 104, 320 (1981).

[17] B.A. Moftah, E. Gete, D.F. Measday, D.S. Armstrong, J. Bauer, T.P. Gorringe, B.L. Johnson, B. Siebels, and S. Stanislaus, Phys. Lett. B 395, 157 (1997).

[18] V. Brudanin, V. Egorov, T. Filipova, A. Kachalkin, V. Kovalenko, A. Salamatin, Yu. Shitov, I. Štekl, S. Vassiliev, V. Vorobel, Ts. Vylov, I. Yutlandov, Sh. Zaparov, J. Deutsch, R. Prieels, L. Grenacs, J. Rak, and Ch. Briancon, Nucl. Phys. A 587, 577 (1995).

[19] V. Gillet and D.A. Jenkins, Phys. Rev. 140, B32 (1965).

[20] V. Brudanin, V. Egorov, T. Filipova, T. Mamedov, A. Salamatin, Yu. Shitov, Ts. Vylov, I. Yutlandov, Sh. Zaparov, J. Deutsch, R. Prieels, Ch. Briançon, M. Kudoyarov, V. Lobanov, and A. Pasternak, *submitted to Nucl. Phys. A.*

[21] T.S. Kosmas, A. Faessler, F. Šimkovic, and J.D. Vergados, Phys. Rev. C 56, 526 (1997).

[22] E.K. Warburton and D.J. Millener, Phys. Rev. C 39, 1120 (1989).

[23] W.A. Richter, M.G. van der Merwe, R.E. Julies, and B.A. Brown, Nucl. Phys. A 523, 325 (1991).

[24] A. Poves and A.P. Zuker, Phys. Rep. 70, 235 (1981).

[25] J.D. Vergados, Phys. Rep. 133, 1 (1986).

[26] H.E. Haber and G.L. Kane, Phys. Rep. 117, 75 (1985).

[27] S. Ciechanowicz, F.C. Khanna, and E. Truhlik, Proceedings of 7th Conference on Mesons and Light Nuclei '98 (Prague-Pruhonice, Czech Republik 1998), eds. J. Adam *et al.*, World Scientific, Singapore 1998, p. 478.